



ISSN 0975-413X  
CODEN (USA): PCHHAX

Der Pharma Chemica, 2016, 8(2):227-237  
(<http://derpharmachemica.com/archive.html>)

## Experimental and theoretical investigation of sulfadiazine as a corrosion inhibitor for carbon steel in HCl medium

B. El Makrini<sup>1</sup>, M. Larouj<sup>2</sup>, H. Lgaz<sup>1,2</sup>, R. Salghi<sup>1\*</sup>, A. Salman<sup>3\*</sup>, M. Belkhaouda<sup>1</sup>, S. Jodeh<sup>4</sup>, M. Zougagh<sup>5,6</sup> and H. Oudda<sup>2</sup>

<sup>1</sup>Laboratory of Applied Chemistry and Environment, ENSA, Université Ibn Zohr, Agadir, Morocco

<sup>2</sup>Laboratory separation processes, Faculty of Science, University Ibn Tofail, Kenitra, Morocco

<sup>3</sup>Department of computer Science, An-Najah National University, Nablus, Palestine

<sup>4</sup>Department of Chemistry, An-Najah National University, Nablus, Palestine

<sup>5</sup>Regional Institute for Applied Chemistry Research, IRICA, E-13004, Ciudad Real, Spain

<sup>6</sup>Castilla-La Mancha Science and Technology Park, E-02006, Albacete, Spain

---

### ABSTRACT

The inhibiting action of Sulfadiazine (SFD) on the corrosion of mild steel in 1 M hydrochloric acid was examined by different corrosion methods, such as weight loss, potentiodynamic polarization and electrochemical impedance spectroscopy (EIS). The experimental results suggest that this compound is an efficient corrosion inhibitor and the inhibition efficiency increases with the increase in inhibitor concentration. Adsorption of this compound on mild steel surface obeys Langmuir's isotherm. Correlation between quantum chemical calculations and inhibition efficiency of the investigated compound is discussed using the Density Functional Theory method (DFT).

**Keywords:** Mild steel; EIS; Electrochemical calculation; Acid corrosion; DFT

---

### INTRODUCTION

Corrosion affects most of industrial sector and may cost billions of dollars each year for preventing and replacement of maintenance[1]–[3]. The use of inhibitors is one of the most effective ways to prevent corrosion. Corrosion inhibitors will reduce the rate of either anodic oxidation or cathodic reduction or both. This will give us anodic, cathodic or mixed type of inhibition[4]–[6]. These compounds can be adsorbed on metal surfaces, block the active sites, and decrease the corrosion rate. The adsorption ability of inhibitors onto the metal surface depends on the nature and surface charge of metal, chemical composition of electrolytes, and molecular structure and electronic characteristics of inhibitor molecules. Most of the potential corrosion inhibitor possess an active heteroatoms such as (N, O, and S), heterocyclic compound and  $\pi$  electron[6]–[10].

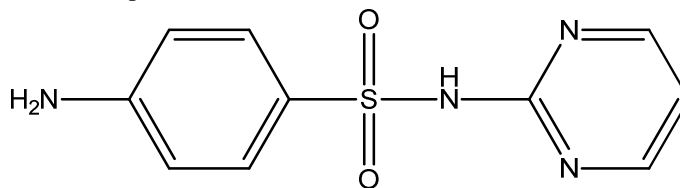
In the recent times, the use of quantum chemical methods in the estimation of potential corrosion inhibitors has been extremely useful. Quantum chemical parameters which are based on the Density Functional Theory such as chemical hardness, electronegativity, chemical potential, nucleophilicity, electrophilicity have been the guide for investigating the agreement with experimental data of the results of computational chemistry works[8], [10]–[13].

In this study, we aimed to investigate the inhibition efficiency of SFD using electrochemical techniques, and weight loss measurements. The choice of this compound as an inhibitor was based on molecular structure considerations. SFD molecule has nitrogen atoms, sulfur and oxygen atoms, which are assumed to be an active center of adsorption.

## MATERIALS AND METHODS

### 2.1. Work electrode and electrolyte

The chemical structure of inhibitor is presented in schematic 1.



schematic1. Chemical structure of Sulfadiazine

The corrosive medium used for all experiments is hydrochloride acid solution of concentration equal to 1.0 M prepared by dilution of an analytical grade 37% HCl with deionized water. The concentration for each tested inhibitor varying from  $10^{-6}$  to  $10^{-3}$  mol/L. The carbon steel specimens employed in this study possess the following composition: 0.370 % C, 0.230 % Si, 0.680 % Mn, 0.016 % S, 0.077 % Cr, 0.011 % Ti, 0.059 % Ni, 0.009 % Co, 0.160 % Cu, and Fe balance. The carbon steel samples used for electrochemical tests were covered in epoxy resin with an exposed surface of  $0.5 \text{ cm}^2$  to the corrosive medium, for gravimetric measurement the coupons with dimensions of  $2.5 \text{ cm} \times 2.5 \text{ cm} \times 0.5 \text{ cm}$  were employed. Prior to each experiment, a freshly prepared solution was used and the sample was mechanically abraded with different emery papers up to 1200 grade, washed with double distilled water followed by acetone and finally dried in room temperature.

### 2.2. Electrochemical Measurements

A Potentiostat / Galvanostat PGZ 100 with Voltmaster 4 software are used for the electrochemical impedance spectra and polarization techniques using three electrode cell in which the reference electrode is a saturated calomel electrode (SCE), the counter electrode made of platinum and the working electrode is carbon steel. After stabilization of studied system at open-circuit potential during 30 min immersion, the electrochemical impedance spectroscopy tests were realized at free potential in the frequency range of 100 kHz to 10 mHz with amplitude of the voltage perturbation is 5 mV AC. For potentiodynamic polarization tests, the electrochemical behavior of carbon steel specimen in the corrosive medium in the presence and absence of inhibitor was performed by scanning the potential from  $-800$  to  $-200$  mV/SCE with a scan rate of 1 mV/s.

### 2.3. Weight loss measurements

The prepared carbon steel electrodes were immersed in aggressive solution with and without the addition of different concentrations of each inhibitor at fixed immersion time of 6 h at 303 K. For each condition, triplicate experiments were performed and the reported weight losses are calculated by average values. For weighing accurately the samples after and before immersion the digital balance with high sensitivity is used.

### 2.4. Theoretical calculations

Quantum chemical methods are usually used to explore the relationship between the inhibitor molecular properties and its corrosion inhibition efficiency[14]–[16]. With these methods, the capability of inhibitor molecules to donate or accept electrons can be predicted with analysis of global reactivity parameters, such as energy gap ( $\Delta E$ ) between HOMO and LUMO, dipole moment ( $\mu$ ), total energy (TE), electron negativity ( $\chi$ ), hardness ( $\eta$ ), softness ( $\sigma$ ), the fraction of electrons transferred ( $\Delta N$ ), etc. The quantum chemical calculations were carried out with geometrically optimized molecules using Gaussian03, E.01 package[17]. The molecular structures were optimized using the functional hybrid B<sub>3</sub>LYP density function theory (DFT) formalism having electron basis set 6-31G (d, p) for all atoms[18]–[20]. According to Koopman's theorem[21], [22], the ionization potential (IE) and electron affinity (EA) of the inhibitors are calculated using the following equations.

$$IE = -E_{\text{HOMO}} \quad (1)$$

$$AE = -E_{\text{LUMO}} \quad (2)$$

Thus, the values of the electronegativity ( $\chi$ ) and the chemical hardness ( $\eta$ ) according to Pearson, operational and approximate definitions can be evaluated using the following relations[23]:

$$\chi = \frac{IE + EA}{2} \quad (3)$$

$$\eta = \frac{IE - EA}{2} \quad (4)$$

The number of transferred electrons ( $\Delta N$ ) was also calculated depending on the quantum chemical method [24]–[26] by using the equation:

$$\Delta N = \frac{\chi_{Fe} - \chi_{inh}}{2(\eta_{Fe} + \eta_{inh})} \quad (5)$$

Where  $\chi_{Fe}$  and  $\chi_{inh}$  denote the absolute electronegativity of iron and inhibitor molecule  $\eta_{Fe}$  and  $\eta_{inh}$  denote the absolute hardness of iron and the inhibitor molecule respectively. In this study, we use the theoretical value of  $\chi_{Fe} = 7.0 \text{ eV mol}^{-1}$  and  $\eta_{Fe} = 0 \text{ eV mol}^{-1}$ , for calculating the number of electron transferred.

## RESULTS AND DISCUSSION

### 3.1. Polarization results

Fig. 2 shows anodic and cathodic polarization plots recorded on mild steel in 1 M HCl in absence and presence of different concentrations of inhibitor. Electrochemical corrosion parameters, such as corrosion potential  $E_{corr}$ , cathodic Tafel slopes  $\beta_c$ , the corrosion current density  $i_{corr}$  and inhibition efficiency  $\eta_p$  (%) are given in Table 1. The percentage of inhibition efficiency  $\eta_p$  was calculated following this equation:

$$\eta_p \% = \left( \frac{i_{corr}^0 - i_{corr}}{i_{corr}^0} \right) \times 100 \quad (6)$$

where  $i_{corr}^0$  and  $i_{corr}$  are the corrosion current densities in the absence and presence of the inhibitor, respectively.

Table 1. Polarization data of carbon steel in 1.0 M HCl without and with various concentrations of SFD at 303 K

Inhibitor	Conc (M)	$-E_{corr}$ (mV/SCE)	$-\beta_c$ (mV dec <sup>-1</sup> )	$I_{corr}$ ( $\mu\text{A cm}^{-2}$ )	$\eta_p$ (%)	$\Theta$
Blank	-	496	162	564.0	-	-
SFD	$5.10^{-3}$	481	171	58.4	89.64	0.8964
	$1.10^{-3}$	488	166	135.2	76.03	0.7603
	$5.10^{-4}$	490	158	178.4	68.37	0.6837
	$1.10^{-4}$	491	160	243.9	56.75	0.5675

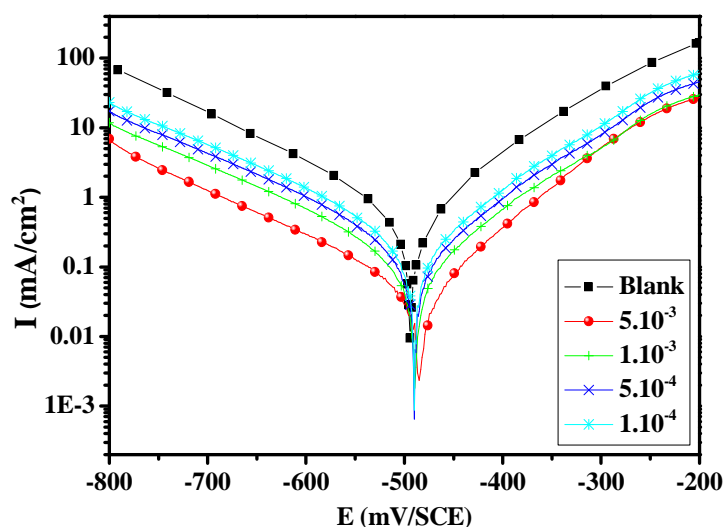


Fig2. Polarisation curves of carbon steel in 1.0 M HCl for various concentrations of SFD at 303K

The shift in  $E_{corr}$  values of the inhibited system compared to the acid blank is less than 80 mV, suggesting that the studied SFD is mixed type inhibitor, inhibit both the anodic dissolution of mild steel and the cathodic  $H^+$  ion

reduction[27]. The values of the anodic cathodic ( $\beta_c$ ) Tafel slopes do not show any uniform trend but change in the anodic and cathodic directions, which again confirms mixed type inhibition mechanism of the studied inhibitor[11]. The decrease of the corresponding current densities with increasing inhibitor concentration is due to the formation of protective films on the electrode surface[26]. The inhibition efficiency ( $\eta_p$  %) increases with increase in concentration for the studied compound, the inhibitor molecules are first adsorbed on the mild steel surface, blocking the available reaction sites, and decrease the corrosion current density.

### 3.2. Electrochemical impedance spectroscopy measurements

The experimental Nyquist plots for mild steel corrosion in 1.0 M HCl solution in the absence and presence of different concentrations of SFD at 303 K are shown in Fig. 3. The Nyquist plots showed single semicircles with one time constant. The capacitive loops are not perfect semicircles due to non-homogeneity and roughness of the mild steel surface[28]. The impedance spectra were analyzed by fitting the experimental data to the equivalent circuit model shown in Fig. 4.

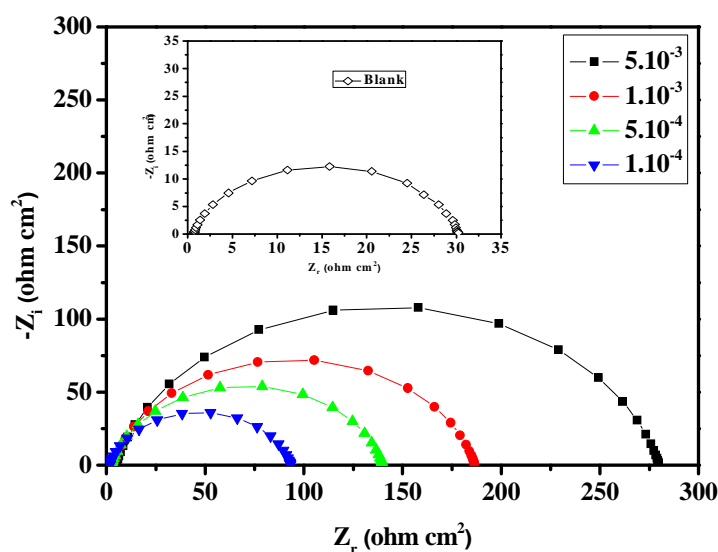


Figure 3. Nyquist diagrams for carbon steel in 1.0 M HCl containing different concentrations of SFD at 303 K

The introduction of CPE into the circuit was necessitated to explain the depression of the capacitance semicircle, which corresponds to surface heterogeneity resulting from surface roughness, impurities, and adsorption of inhibitor[11]. The impedance of this element is frequency-dependent and can be calculated using the Eq. 7[27]:

$$Z_{CPE} = \frac{1}{Q(j\omega)^n} \quad (7)$$

Where Q is the CPE constant (in  $\Omega^{-1}S^n \text{ cm}^{-2}$ ),  $\omega$  is the angular frequency (in  $\text{rad s}^{-1}$ ),  $j^2 = -1$  is the imaginary number and n is a CPE exponent which can be used as a gauge for the heterogeneity or roughness of the surface. The double layer capacitance values ( $C_{dl}$ ) is evaluated from constant phase element CPE (Q, n) and a charge transfer resistance value ( $R_{ct}$ ), using the following relation:

$$C_{dl} = \sqrt[n]{Q \cdot R_{ct}^{1-n}} \quad (8)$$

Where Q is the constant phase element (CPE) and n is a coefficient can be used as a measure of surface inhomogeneity.

Table 2. Impedance parameters for corrosion of carbon steel in 1.0 M HCl in the absence and presence of different concentrations of SFD at 303 K

Inhibitor	Conc (g/L)	$R_{ct}$ ( $\Omega \text{ cm}^2$ )	n	$Q \times 10^{-4}$ ( $\text{s}^n \Omega^{-1} \text{ cm}^{-2}$ )	$C_{dl}$ ( $\mu\text{F cm}^{-2}$ )	$\eta_z$ (%)	$\theta$
Blank	-	29.35	0.91	1.7610	91.63	-	-
	$5.10^{-3}$	279.77	0.84	0.3253	13.29	89.51	0.8951
SFD	$1.10^{-3}$	186.51	0.81	0.4657	15.30	84.26	0.8426
	$5.10^{-4}$	137.7	0.83	0.7698	30.33	78.68	0.7868
	$1.10^{-4}$	91.78	0.87	1.3244	68.52	68.02	0.6802

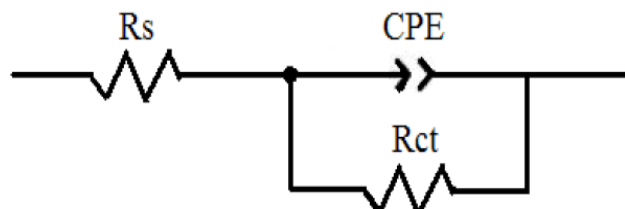


Figure 4. Equivalent electrical circuit corresponding to the corrosion process on the carbon steel in hydrochloric acid

The corresponding electrochemical parameters are presented in Table 2 and reveal that the inhibitor increased the magnitude of  $R_{ct}$ , with corresponding decrease in the double layer capacitance ( $C_{dl}$ ). The increase in  $R_{ct}$  value in inhibited system, which corresponds to an increase in the diameter of the Nyquist semicircle, confirms the corrosion inhibiting effect of inhibitor. The observed decrease in  $C_{dl}$  values, which normally results from a decrease in the dielectric constant and/or an increase in the double-layer thickness, can be attributed to the adsorption of inhibitor molecule (with lower dielectric constant compared to the displaced adsorbed water molecules) onto the metal/electrolyte interface, thereby protecting the metal from corrosive attack[29]–[31].

### 3.3. Weight loss tests

The corrosion parameters such as corrosion rate ( $C_R$ ), surface coverage ( $\theta$ ) and corrosion inhibition efficiency ( $\eta_w\%$ ) obtained by weight loss measurements for mild steel specimen immersed in 1.0 M HCl solution in the absence and presence of different concentration of inhibitor SFD for an immersion period of 6 h at 303K and are listed in Table 3 and presented in Fig. 5. From Table 3, it is apparent that inhibition efficiency increased with increasing concentration of the inhibitor. By increasing the inhibitor concentration, the part of metal surface covered by inhibitor molecule increases and that leads to an increase in the inhibition efficiencies[32].

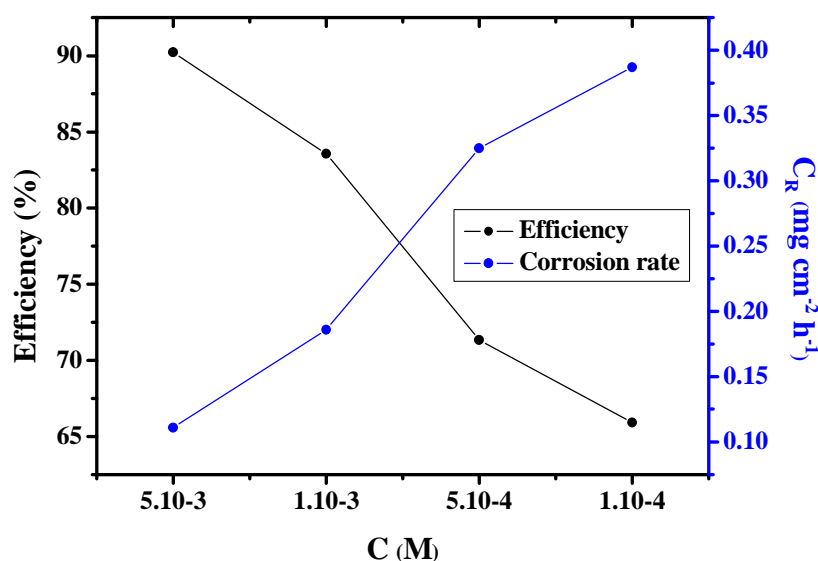


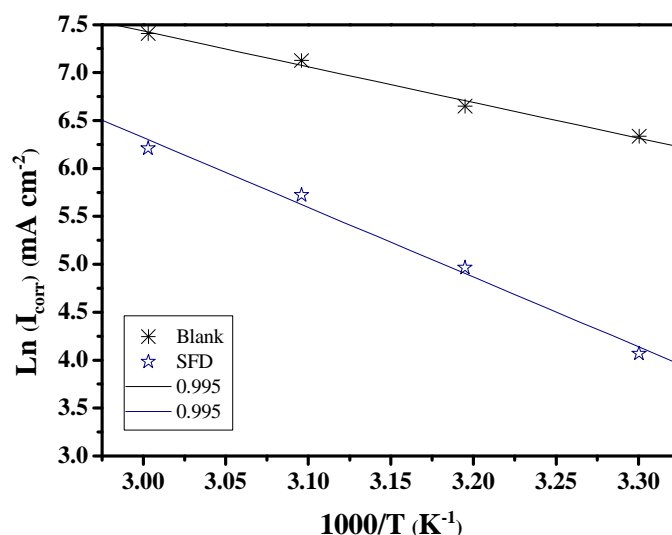
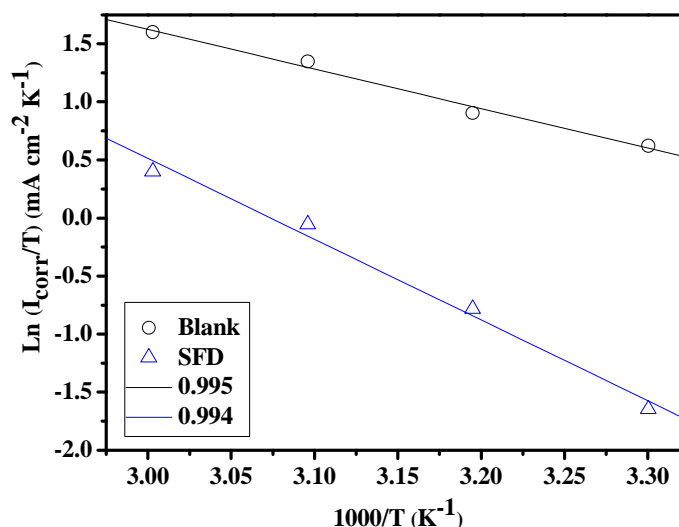
Fig. 5. Relationship between the corrosion rate, the inhibition efficiency and SFD concentrations for steel after 6 h immersion in 1.0 M HCl at 303 K

Table3. Corrosion parameters obtained from weight loss measurements for carbon steel in 1.0 M HCl containing various concentration of SFD at 303 K

Inhibitor	Concentration (g/L)	$C_R$ ( $\text{mg cm}^{-2} \text{h}^{-1}$ )	$\eta_w$ (%)	$\Theta$
Blank	-	1.135	-	-
SFD	$5.10^{-3}$	0.111	90.23	0.9023
	$1.10^{-3}$	0.186	83.56	0.8356
	$5.10^{-4}$	0.325	71.34	0.7134
	$1.10^{-4}$	0.387	65.92	0.6592

### 3.4. Effect of temperature

Effect of temperature on the corrosion of mild steel in 1.0 M HCl without and with various concentrations of the studied inhibitors was investigated between 303 K and 333 K. Corrosion parameters such as corrosion potential  $E_{\text{corr}}$ , cathodic Tafel slopes  $\beta_c$ , the corrosion current density  $i_{\text{corr}}$  and  $\eta_p\%$  obtained from polarization potentiodynamic at optimum concentration and different temperatures are shown in Table 4. It is clear from the Table 4 that the  $i_{\text{corr}}$  increases with increase in temperature in the presence and absence of the inhibitor. The  $\eta_p\%$  decreased with increasing temperature from 303 to 333 K. This type of behavior can be described on the basis that increase in temperature leads to a shift of the equilibrium position of the adsorption/desorption phenomenon towards desorption of the inhibitor molecule at the surface of mild steel [30], [31], [33], [34].

Fig. 6. Arrhenius plots for mild steel in 1.0 M HCl and 1.0 M HCl +  $5.10^{-3}$  M SFDFig. 7. Transition state plots for mild steel in 1.0 M HCl and 1.0 M HCl +  $5.10^{-3}$  M SFD

In order to calculate the activation energy for the corrosion reaction, the Arrhenius Eq. 9 was used[35], [36]:

$$C_R = k \exp\left(\frac{-E_a}{RT}\right) \quad (9)$$

Where  $C_R$  is the corrosion rate,  $R$  the gas constant,  $T$  the absolute temperature,  $A$  the pre-exponential factor, The apparent activation energies ( $E_a$ ) and pre-exponential factors ( $k$ ) at  $5.10^{-3}$  M of inhibitor are calculated by linear regression between  $\ln(I_{\text{corr}})$  and  $1/T$  (Fig. 6), and also the results shown in Table 5. It is evident from Table 5 that the value of the apparent activation energy for the inhibited solution were higher than that for the uninhibited solution, indicating that the dissolution of mild steel was decreased due to formation of a barrier by the adsorption of the inhibitors on metal surface[37].

**Table 4.**The influence of temperature on the electrochemical parameters for carbon steel electrode immersed in 1.0 M HCl and 1.0 M HCl +  $5.10^{-3}$  M SFD

Inhibitor	Temp (K)	$-E_{\text{corr}}$ (mV/SCE)	$-\beta c$ (mV dec $^{-1}$ )	$I_{\text{corr}}$ ( $\mu\text{A cm}^{-2}$ )	$\eta_{\text{Tafel}}$ (%)
Blank	303	496	162.5	564	-
	313	498	154.5	773	-
	323	492	176.0	1244	-
	333	497	192.0	1650	-
SFD	303	481	171.0	58.4	89.64
	313	487	166.7	143.2	81.47
	323	488	173.4	305.7	75.43
	333	486	163.7	497.8	69.83

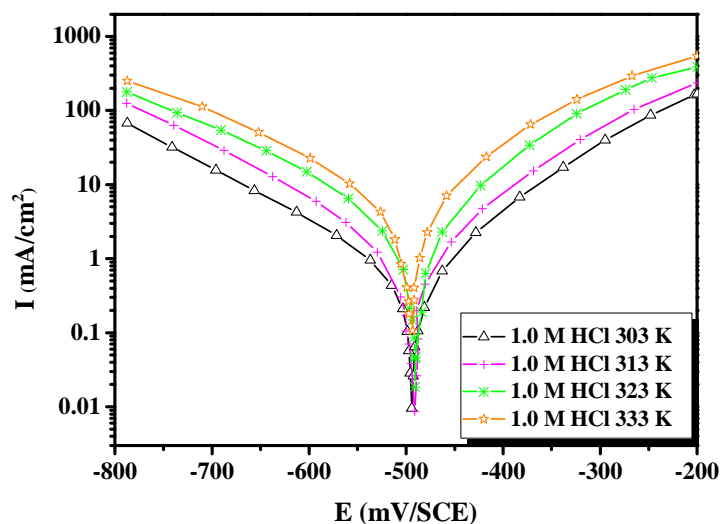


**Fig. 8.**Potentiodynamic polarisation curves of carbon steel in 1.0 M HCl at different temperatures

Other activation parameters can be evaluated from the effect of temperature. Enthalpy and entropy of activation were calculated using the alternative form of Arrhenius[38]–[40]Eq. 10:

$$C_R = \frac{RT}{Nh} \exp\left(\frac{\Delta S_a}{R}\right) \exp\left(-\frac{\Delta H_a}{RT}\right) \quad (10)$$

Where,  $h$  is the Planck's constant,  $N$  is the Avogadro's number,  $R$  is the molar gas constant and  $T$  is the absolute temperature. Straight lines were obtained with a slope and an intercept (Fig. 7) from which the activation thermodynamic parameters  $\Delta H_a$  and  $\Delta S_a$  were calculated, as listed in Table 5. The negative value of  $\Delta S^*$  for inhibitor indicate that the formation of the activated complex in the rate determining step represents an association rather than a dissociation step, meaning that a decrease in disorder takes place during the course of the transition from reactants to activated complex[41], [42].

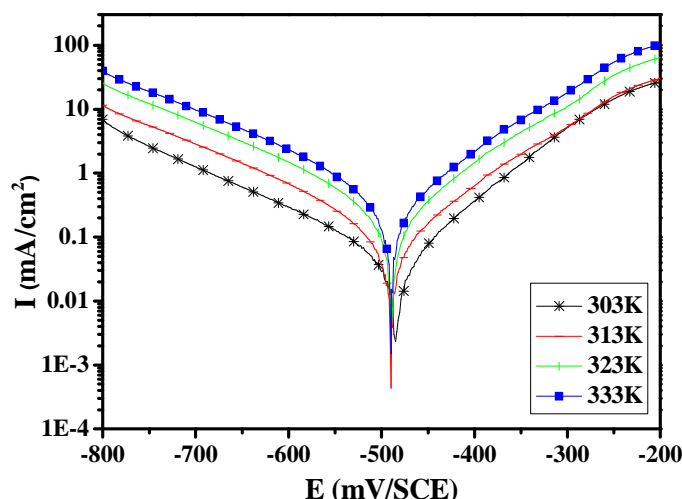


Fig. 9. Potentiodynamic polarisation curves of carbon steel in 1.0 M HCl in the presence of  $5.10^{-3}$  M SFD at different temperatures

Table 5. Corrosion kinetic parameters for mild steel in 1.0 M HCl in the presence and absence of SFD

Inhibitor	$E_a$ (kJ/mol)	$\Delta H_a$ (kJ/mol)	$\Delta S_a$ (J mol <sup>-1</sup> K <sup>-1</sup> )	$E_a - \Delta H_a$
Blank	31.00	28.35	-98.80	2.65
SFD	60.44	57.80	-19.69	2.64

### 3.5. Adsorption considerations

Information on the interaction between the inhibitor molecules and the mild steel surface can be provided by adsorption isotherm. Plotting  $C_{inh}/\theta$  vs.  $C_{inh}$  yielded a straight line (Fig. 10) with a slope value given in Table 6 at different temperatures. The  $R^2$  and slope value are near to unity indicating that the adsorption of these inhibitors obeys the Langmuir adsorption isotherm represented by the following equation.

$$\frac{C_{inh}}{\theta} = \frac{1}{K_{ads}} + C_{inh} \quad (11)$$

Where, C is the concentration of the inhibitor,  $K_{ads}$  is the equilibrium constant of adsorption and  $\theta$  is the surface coverage.

The values of  $K_{ads}$  were calculated from the intercept of Fig. 10. Large value of  $K_{ads}$  were obtained for studied inhibitor suggesting more efficient adsorption and hence better corrosion inhibition efficiency. Using the values of  $K_{ads}$ , the values of  $\Delta G_{ads}$  were obtained by using the following equation:

$$\Delta G_{ads}^0 = -RT \ln(K * 55.5) \quad (12)$$

Where the value 55.5 is the water concentration in solution expressed in mol.L<sup>-1</sup>.

The calculated value of  $K_{ads}$  and  $\Delta G_{ads}$  are listed in Table 6. In general, values of  $\Delta G_{ads}$  up to  $-20$  kJmol<sup>-1</sup> are compatible with physisorption and those which are more negative than  $-40$  kJmol<sup>-1</sup> involve chemisorptions[11], [12]. The calculated  $\Delta G_{ads}$  values for SFD were found in  $-32.0$  kJmol<sup>-1</sup>, at different temperatures (303–333) K, this value were between the threshold values for physical adsorption and chemical adsorption, indicating that the adsorption process of inhibitor at mild steel surface involve both the physical as well as the chemical adsorption[11], [36], [43].



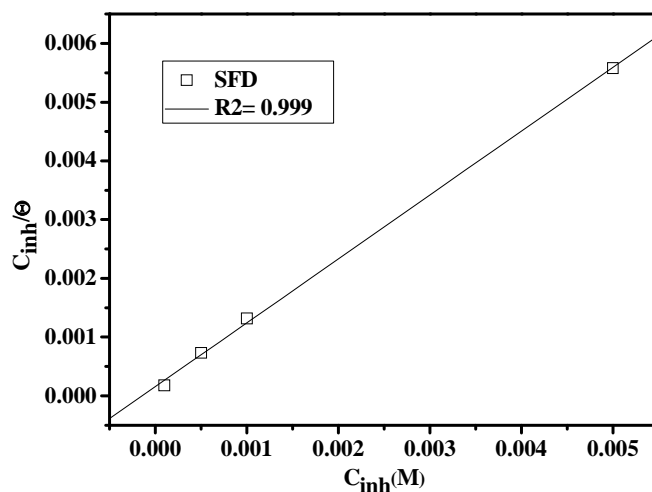


Figure 10. Langmuir adsorption of SFD on the carbon steel surface in 1.0 M HCl solution at 303K

Table 5. Thermodynamic parameters for the adsorption of H1 in 1.0 M HCl on the mild steel at 303K

Inhibitor	Slope	$K_{ads}(M^{-1})$	$\Delta G^*_{ads}(kJ/mol)$
SFD	1.086427	3532.19	

### 3.6. Quantum Chemical Calculations

The structure and electronic parameters were obtained by means of theoretical calculations using the computational methodologies of quantum chemistry. The optimized molecular structures and frontier molecular orbital density distribution of the studied molecule are shown in Figure 11. The calculated quantum chemical parameters such as  $E_{HOMO}$ ,  $E_{LUMO}$ ,  $\Delta E_{LUMO-HOMO}$ , dipole moment ( $\mu$ ) and  $\Delta N$  are listed in Table 6.

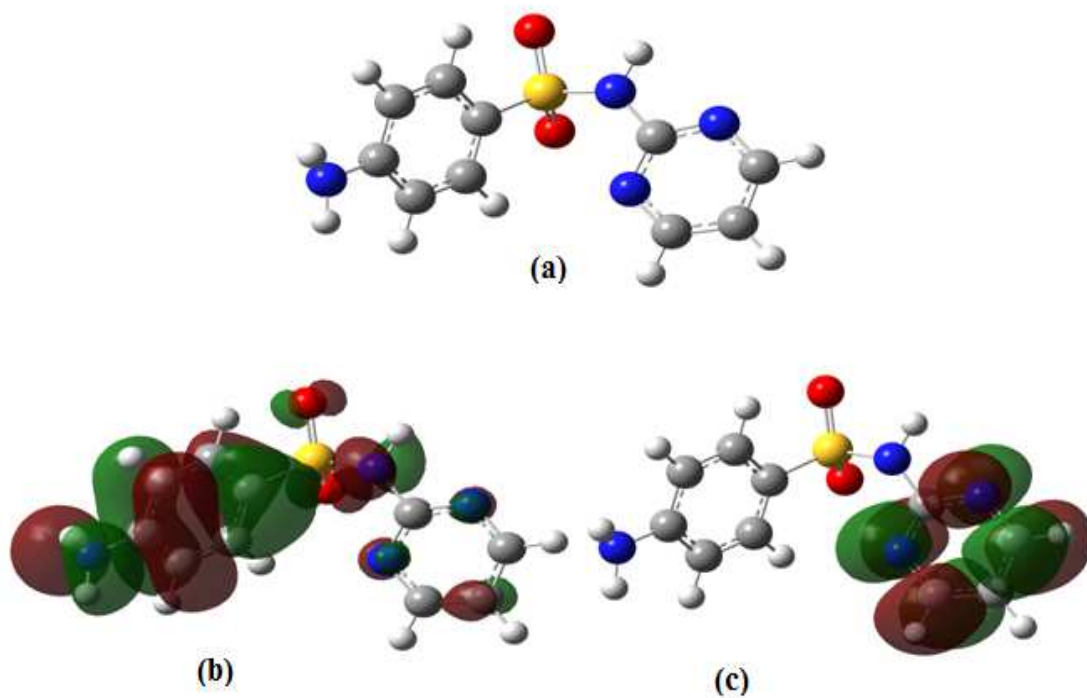


Fig.11. (a) Optimized molecular structure (b) HOMO and (c) LUMO molecular orbital density distribution of SFD

Table7. Quantum chemical parameters for SFD calculated using B3LYP/ 6-31G (d,p)

	$E_{\text{HOMO}}$ (eV)	$E_{\text{LUMO}}$ (eV)	$\Delta E_{\text{gap}}$ (eV)	$\mu$ (debye)	TE (eV)	$\chi$ (eV)	$\eta$ (eV)	$\Delta N$
SFD	-5.98079	-1.16791	4.81288	7.2045	-31429	3.574	2.406	0.712

$E_{\text{HOMO}}$  is often associated with the electron-donating ability of a molecule and its high value (-5.98079) is likely to indicate a tendency to donate electrons to appropriate low-energy acceptor states. Increasing values of the  $E_{\text{HOMO}}$  facilitate adsorption (and therefore inhibition) by influencing the transport process through the adsorbed layer.  $E_{\text{LUMO}}$  indicates the ability of the molecule to accept electrons; hence these are the acceptor states. The lower the value (-1.04954eV) of  $E_{\text{LUMO}}$ , the more probable it is that the molecule would accept electrons [44]. For the dipole moment ( $\mu$ ), higher value (7.2045) of  $\mu$  will favor a strong interaction of inhibitor molecules to the metal surface [45].

The fraction of electrons transferred from inhibitor to the iron molecule ( $\Delta N$ ) was calculated. According to other reports [46, 47], value of  $\Delta N$  showed inhibition effect resulted from electron donation. In this study, the SFD was the donors of electrons while the carbon steel surface was the acceptor. The SFD was bound to the carbon steel surface, and thus formed inhibition adsorption layer against corrosion.

## CONCLUSION

The SFD act as good corrosion inhibitor for mild steel in 1.0 M HCl solution. Polarization studies showed that the tested inhibitor is mixed type in nature. EIS measurements show that charge transfer resistance ( $R_{\text{ct}}$ ) increases and double layer capacitance ( $C_{\text{dl}}$ ) decreases in the presence of inhibitor, which suggested the adsorption of the inhibitor molecules on the surface of mild steel. The results obtained from Langmuir adsorption isotherm suggested that the mechanism of corrosion inhibition is occurring mainly through adsorption process. Quantum chemical results of SFD indicating that the inhibitor is good corrosion inhibitor for mild steel in 1.0 M HCl solution.

## Acknowledgment

The authors would like to thank MENA NWC for their financial support for grant no: WIF 04. Also, we would like to extend our thanks to Palestine Water Authority (PWA) and MEDRIC for their support. The support given through an "INCRECYT" research contract to M. Zougagh is also acknowledged.

## REFERENCES

- [1] D. B. Hmamou, R. Salghi, A. Zarrouk, H. Zarrouk, M. Errami, B. Hammouti, L. Afia, L. Bazzi, et L. Bazzi, *Res. Chem. Intermed.*, **2013**, 39, 973-989.
- [2] M. Larouj, H. Lgaz, S. Houda, H. Zarrok, H. Bourazmi, A. Zarrouk, A. Elmidaoui, A. Guenbour, S. Boukhris, et H. Oudda, *Journal of Materials and Environmental Science*, **2015**, 3251-3267.
- [3] L. Afia, R. Salghi, L. Bammou, E. Bazzi, B. Hammouti, L. Bazzi, et A. Bouyanzer, *J. Saudi Chem. Soc.*, **2014**, 18, 19-25.
- [4] T. Ghazouani, D. B. Hmamou, E. Meddeb, R. Salghi, O. Benali, H. Bouya, B. Hammouti, et S. Fattouch, *Res. Chem. Intermed.*, 1-18.
- [5] O. Ouachikh, A. Bouyanzer, M. Bouklah, J.-M. Desjobert, J. Costa, *Surf. Rev. Lett.*, **2009** 16, 49-54.
- [6] L. Afia, R. Salghi, E. H. Bazzi, A. Zarrouk, B. Hammouti, M. Bouri, H. Zarrouk, L. Bazzi, et L. Bammou, *Res. Chem. Intermed.*, **2012**, 38, 1707-1717.
- [7] D. B. Hmamou, R. Salghi, A. Zarrouk, O. Benali, F. Fadel, H. Zarrok, et B. Hammouti, *Int. J. Ind. Chem.*, 2012, 3, 1-9.
- [8] H. Zarrok, A. Zarrouk, B. Hammouti, R. Salghi, C. Jama, et F. Bentiss, *Corros. Sci.*, **2012**, 64, 243-252.
- [9] L. Afia, R. Salghi, A. Zarrouk, H. Zarrok, E. H. Bazzi, B. Hammouti, et M. Zougagh, *Trans. Indian Inst. Met.*, **2013**, 66, 43-49.
- [10] E. H. A. Addi, L. Bazzi, M. Hilali, E. A. Zine, R. Salghi, et S. E. Issami, *Can. J. Chem.*, **2003**, 81, 297-306.
- [11] R. N. Singh, A. Kumar, R. K. Tiwari, P. Rawat, *Spectrochim. Acta. A. Mol. Biomol. Spectrosc.*, **2013**, 112, 182-190.
- [12] H. Jafari, I. Danaee, H. Eskandari, et M. Rashvand Avei, *J. Mater. Sci. Technol.*, **2014**, 30, 239-252.
- [13] L. M. Rodríguez-Valdez, W. Villamizar, M. Casales, J. G. González-Rodríguez, A. Martínez-Villafañe, L. Martínez, et D. Glossman-Mitnik, *Corros. Sci.*, **2006**, 48, 4053-4064.
- [14] I. Lukovits, E. Kalman, F. Zucchi, *Corrosion*, **2001**, 57, 3-8.
- [15] R. G. Parr, W. Yang, *J. Am. Chem. Soc.*, **1984**, 106, 4049-4050.
- [16] I. B. Obot, D. D. Macdonald, et Z. M. Gasem, *Corros. Sci.*, **2015**, 99, 1-30.
- [17] M. J. Frisch et al., GAUSSIAN 03, Revision B.03, Gaussian, Inc., Wallingford, CT, **2004**.
- [18] C. Lee, W. Yang, et R. G. Parr, *Phys. Rev. B*, **1988**, 37, 785-789.

- [19] N. A. Wazzan, *J. Ind. Eng. Chem*, **2015**, 26, 291-308.
- [20] I. Danaee, O. Ghasemi, G. R. Rashed, M. Rashvand Avei, et M. H. Maddahy, *J. Mol. Struct*, **2013**, 1035, 247-259.
- [21] L. Feng, H. Yang, et F. Wang, *Electrochimica Acta*, **2011**, 58, 427-436.
- [22] X. Li, S. Deng, et X. Xie, *J. Taiwan Inst. Chem. Eng*, **2014**, 45, 1865-1875.
- [23] K. Ramya, R. Mohan, K. K. Anupama, et A. Joseph, *Mater. Chem. Phys*, **2015**, 149-150, 632-647.
- [24] K. F. Khaled, *Corros. Sci*, **2011**, 3, 3457-3465.
- [25] S. RameshKumar, I. Danaee, M. RashvandAvei, et M. Vijayan, *J. Mol. Liq*, **2015**, 212, 168-186.
- [26] L. O. Olasunkanmi, M. M. Kabanda, et E. E. Ebenso, *Phys. E Low-Dimens. Syst. Nanostructures*, **2016**, 76, 109-126.
- [27] C. Verma, M. A. Quraishi, et A. Singh, *J. Mol. Liq*, **2015**, 212, 804-812.
- [28] C. B. Verma, M. A. Quraishi, et A. Singh, *J. Taiwan Inst. Chem. Eng*, **2015**, 49, 229-239.
- [29] N. A. Odewunmi, S. A. Umoren, et Z. M. Gasem, *J. Environ. Chem. Eng*, **2015**, 3, 286-296.
- [30] P. Singh, A. Singh, et M. A. Quraishi, *J. Taiwan Inst. Chem. Eng*.
- [31] N. O. Eddy, H. Momoh-Yahaya, et E. E. Oguzie, *J. Adv. Res.*, **2015**, 6, 203-217, 2015.
- [32] K. R. Ansari et M. A. Quraishi, *J. Ind. Eng. Chem*, **2014**, 20, 2819-2829.
- [33] D. Zhang, Y. Tang, S. Qi, D. Dong, H. Cang, et G. Lu, *Corros. Sci*, **2016**, 102, 517-522.
- [34] M. H. Hussin, A. A. Rahim, M. N. Mohamad Ibrahim, et N. Brosse, *Measurement*, **2016**, 78, 90-103
- [35] C. Verma, P. Singh, et M. A. Quraishi, *J. Assoc. Arab Univ. Basic Appl. Sci*.
- [36] C. Verma, M. A. Quraishi, et A. Singh, *J. Taiwan Inst. Chem. Eng*, **2016**, 58, 127-140.
- [37] D. B. Hmamou, R. Salghi, A. Zarrouk, M. R. Aouad, O. Benali, H. Zarrok, M. Messali, B. Hammouti, M. M. Kabanda, et M. Bouachrine, *Ind. Eng. Chem. Res*, **2013**, 52, 14315-14327.
- [38] L. Bammou, B. Chebli, R. Salghi, L. Bazzi, B. Hammouti, M. Mihit, et H. Idrissi, *Green Chem. Lett. Rev*, **2010**, 3, 173-178.
- [39] M. Mihit, S. El Issami, M. Bouklah, L. Bazzi, B. Hammouti, E. Ait Addi, R. Salghi, et S. Kertit, *Appl. Surf. Sci*, **2006**, 252, 2389-2395.
- [40] O. I. El Mouden, A. Anejjar, M. Messali, R. Salghi, H. A. Ismat, et B. Hammouti, *Chem Sci Rev Lett*, **2014**, 3, 579-588.
- [41] D. B. Hmamou, R. Salghi, A. Zarrouk, B. Hammouti, O. Benali, H. Zarrok, et S. S. Al-Deyab, *Res. Chem. Intermed*, **2013**, 39, 3475-3485.
- [42] K. Barouni, L. Bazzi, R. Salghi, M. Mihit, B. Hammouti, A. Albourine, et S. El Issami, *Mater. Lett*, **2008**, 62, 3325-3327.
- [43] C. Verma, E. E. Ebenso, I. Bahadur, I. B. Obot, et M. A. Quraishi, *J. Mol. Liq*, **2015**, 212, 209-218.
- [44] M. Lebrini, M. Lagrenee, M. Traisnel, L. Gengembre, H. Vezin, F. Bentiss, *Appl. Surf. Sci*, **2007**, 253, 9267.
- [45] S. Vijayakumar, P. Kolandaivel, *J. Mol. Struct. S. Vijayakumar, P. Kolandaivel* *J. Mol...Struct*, **2006** 770 23-29.
- [46] S. Xia, M. Qui, L. Yu, F. Lui, *Corros. Sci* 50 (2008) 2021.
- [47] H. Ju, Z. Kai, Y. Li, *Corros. Sci* 50 (2008) 865.